The solution structure of human thioredoxin complexed with its target from Ref-1 reveals peptide chain reversal

Jun Qin, G Marius Clore*, W Poindexter Kennedy, John Kuszewski and Angela M Gronenborn*

Background: Human thioredoxin (hTRX) is a 12 kDa cellular redox protein that has been shown to play an important role in the activation of a number of transcriptional and translational regulators via a thiol-redox mechanism. This activity may be direct or indirect via another redox protein known as Ref-1. The structure of a complex of hTRX with a peptide comprising its target from the transcription factor NFκB has previously been solved. To further extend our knowledge of the recognition by and interaction of hTRX with its various targets, we have studied a complex between hTRX and a Ref-1 peptide. This complex represents a kinetically stable mixed disulfide intermediate along the reaction pathway.

Results: Using multidimensional heteronuclear edited and filtered NMR spectroscopy, we have solved the solution structure of a complex between hTRX and a 13-residue peptide comprising residues 59–71 of Ref-1. The Ref-1 peptide is located in a crescent-shaped groove on the surface of hTRX, the groove being formed by residues in the active-site loop (residues 32–36), helix 3, β strands 3 and 5, and the loop between β strands 3 and 4. The complex is stabilized by numerous hydrogen-bonding and hydrophobic interactions that involve residues 61–69 of the peptide and confer substrate specificity.

Conclusions: The orientation of the Ref-1 peptide in the hTRX–Ref-1 complex is opposite to that found in the previously solved complex of hTRX with the target peptide from the transcription factor NFκB. Orientation is determined by three discriminating interactions involving the nature of the residues at the P_{-2}, P_{-4} and P_{-5} binding positions. (P_0 defines the active cysteine of the peptide, Cys65 for Ref-1 and Cys62 for NFκB. Positive and negative numbers indicate residues N-terminal and C-terminal to this residue, respectively, and vice versa for NFκB as it binds in the opposite orientation.) The environment surrounding the reactive Cys32 of hTRX, as well as the packing of the P_{+3} to P_{-4} residues are essentially the same in the two complexes, despite the opposing orientation of the peptide chains. This versatility in substrate recognition permits hTRX to act as a wide-ranging redox regulator for the cell.

Address: Laboratory of Chemical Physics, Building 5, National Institute of Diabetes and Digestive and Kidney Diseases, National Institutes of Health, Bethesda, MD 20892-0520, USA.

*Corresponding authors. E-mail: GMC, clore@vger.niddk.nih.gov; AMG, gronenborn@vger.niddk.nih.gov

Introduction

Thioredoxin is an oxido-reductase [1,2] that has been shown to play a key role in the activation of a number of transcriptional [3–10] and translational [11–12] regulators. It operates via a thiol-redox mechanism involving the reduction of specific cysteine residues of the substrate. This activity may be direct, as in the case of NFκB [3–5] and the psbA mRNA protein complex [11,12], or indirect via another redox protein known as Ref-1 [8,9]. The solution structure of human thioredoxin (hTRX) in an intermolecular (otherwise known as mixed) disulfide complex with a peptide comprising its target site from the transcription factor NFκB showed that the complex is stabilized by numerous interactions that confer substrate specificity [12]. We now present the solution structure of hTRX in a complex with a peptide comprising its target site from Ref-1, and show that the binding orientation of the Ref-1 peptide is opposite to that of the NFκB peptide. Thus, hTRX illustrates novel principles of flexible substrate recognition that permit disulfide-bond reduction of a wide variety of target proteins.

Redox control of the DNA-binding activity of the transcription factor AP-1 (a heterodimer of fos and jun) by Ref-1 is stimulated by the thioredoxin/thioredoxin reductase system [8,9]. The region essential for Ref-1 redox activity has been localized to the N terminus of the protein, and site-directed mutagenesis has identified the cysteine at position 65 as the redox active site [13,14]. Upon oxidation, Ref-1 becomes redox inactive and is no longer able to activate AP-1. The activity of Ref-1 is restored by hTRX [8,9,13,14]. Indeed, a direct physical

Figure 1
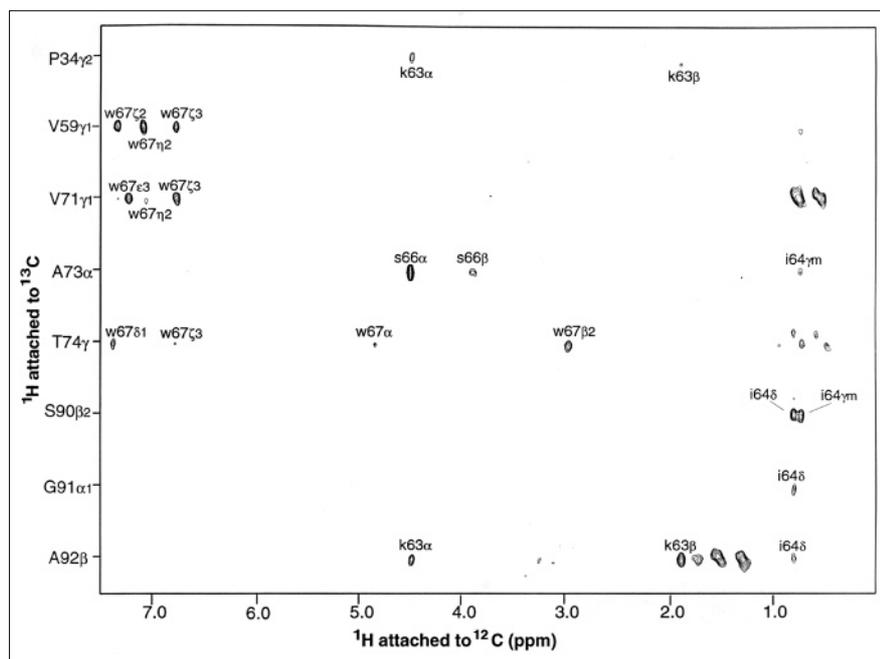
Composite of ^{13}C-^1H strips taken from the 120 ms mixing time 600 MHz 3D $^{13}C(F_2)$-edited/$^{12}C(F_3)$-filtered NOE spectrum of the hTRX–Ref-1 peptide complex, illustrating NOEs between protons of the unlabeled peptide (attached to ^{12}C along the F_3 axis) and protons of labeled hTRX (attached to ^{13}C). Residues of hTRX and the Ref-1 peptide are indicated by upper-case and lower-case letters, respectively.

and functional interaction between Ref-1 and human thioredoxin has been demonstrated both *in vivo* and *in vitro* using the yeast two hybrid system, cross-linking, and surface plasmon resonance (J Yodoi, personal communication). We have investigated this interaction at the atomic level by solving the three-dimensional (3D) structure of a complex of human thioredoxin with a peptide comprising the relevant target site from Ref-1.

Results and discussion
Structure determination
The mixed disulfide intermediate was formed by reacting the quadruple (Cys35→Ala, Cys62→Ala, Cys69→Ala and Cys73→Ala) mutant of hTRX with a 13-residue peptide comprising residues 59–71 of Ref-1 and purifying the resulting complex by HPLC. The Cys62→Ala, Cys69→Ala and Cys73→Ala mutations prevent any problems associated with the formation, upon oxidation, of intermolecular disulfide bonds upon oxidation involving the three non-active-site cysteine residues [15]. The Cys35→Ala mutation ensures that the reaction does not proceed beyond the mixed disulfide intermediate (Cys35 acts as the resolving sulfhydryl anion in the native complex) [12]. The intermolecular disulfide bond is formed between the two reactive cysteines, Cys32 of hTRX [1] and Cys65 of Ref-1 [13]. The solution structure was solved by multidimensional heteronuclear-edited and -filtered NMR spectroscopy making use of isotopically labelled hTRX (^{15}N and $^{15}N/^{13}C$) and the Ref-1 peptide at natural isotopic abundance [16–18]. The structure determination was based on a total of 3663 experimental NMR restraints, including 55 intermolecular

interproton distance restraints. An example of the quality of the experimental data is shown in Figure 1. This illustrates strips taken from the 3D ^{13}C-edited(F_2)/$^{12}C(F_3)$-filtered nuclear Overhauser enhancement (NOE) spectrum, showing intermolecular contacts between ^{13}C-attached protons of hTRX and ^{12}C-attached protons of the unlabeled Ref-1 peptide. A summary of the structural statistics is provided in Table 1, and a superposition of the final 35 structures is shown in Figure 2. The structure is well defined with a precision (excluding residues 59–60 and 70–71 of the peptide which are disordered and do not interact with hTRX) of 0.24±0.02 Å for the backbone atoms, 0.29±0.34 Å for all ordered atoms and 0.50±0.03 Å for all atoms (Table 2). 92% of the residues lie in the most favoured regions of the Ramachandran plot, and the remaining 8% are in the additional allowed regions [19]. The backbone rms difference for the protein between its mean coordinates in the hTRX–Ref-1 complex and those in the hTRX–NFκB complex [12], oxidized hTRX and reduced hTRX [15], are 0.62, 0.72 and 0.75 Å, respectively.

Description of the complex
A detailed view of the interactions between the peptide and hTRX is shown in Figure 3. To facilitate discussion we denote the residue numbering of the Ref-1 peptide as follows: P_0 represents the disulfide-bonded cysteine, and positive and negative numbers indicate residues N-terminal and C-terminal to this cysteine, respectively. (Note that in the complex with the NFκB peptide [12], positive and negative numbers indicate residues C-terminal and N-terminal to the disulfide-bonded cysteine, respectively,

Table 1

Structural statistics.*

Structural statistics	<SA>	($\overline{SA}$)r
Rms deviations from exptl distance restraints (Å)[†]		
All (2617)	0.036±0.035	0.035
Intramolecular hTRX interproton distances		
interresidue sequential (|i–j|=1) (534)	0.030±0.002	0.029
interresidue short range (1<|i–j|≤5) (539)	0.048±0.002	0.047
interresidue long range ((|i–j|)>5) (688)	0.036±0.002	0.034
intraresidue (682)	0.016±0.002	0.018
Intramolecular Ref-1 peptide		
interproton distances (83)	0.036±0.006	0.034
Intermolecular hTRX-Ref1		
interproton distances (55)	0.062±0.004	0.059
hTRX hydrogen-bond restraints (36)	0.072±0.072	0.055
Rms deviations from $^3J_{HN\alpha}$		
coupling constants (Hz) (86)[†]	0.79±0.02	0.79
Rms deviations from		
exptl dihedral restraints (°) (321)[†,‡]	0.35±0.05	0.37
Rms deviations from exptl secondary shifts (ppm)		
$^{13}C\alpha$ (100)	1.08±0.02	1.07
$^{13}C\beta$ (97)	1.07±0.01	1.08
Rms deviations from exptl ^1H shifts (442)[‡]	0.27±0.002	0.28
Deviations from idealized covalent geometry		
Bonds (Å) (1835)	0.004±0.0001	0.006
Angles (°) (3333)	0.570±0.010	0.684
Impropers (°) (938)[§]	0.476±0.013	0.524
E_{L-J} (kcal mol^{-1})[#]	–568±7	–548

*The notation of the NMR structures is as follows: <SA> is the ensemble comprising the final 35 simulated annealing structures; $\overline{SA}$ is the mean structure obtained by averaging the coordinates of the individual SA structures best fitted to each other (excluding residues 59–60 and 70–71 of the Ref-1 peptide); ($\overline{SA}$)r is the restrained regularized mean structure obtained by restrained regularization of the mean structure $\overline{SA}$ [37]. The number of terms for the various restraints are given in parentheses and apply to the entire complex. [†]None of the structures exhibit distance violations greater than 0.3 Å, dihedral angle violations greater than 5°, or $^3J_{HN\alpha}$ coupling constant violations greater than 2 Hz; there are no systematic interproton distance violations between 0.1 and 0.3 Å among the ensemble of calculated structures. [‡]The dihedral angle restraints comprise 104 φ, 76 ψ, 78 χ$_1$ and 30 χ$_2$ angles for hTRX, and 11 φ, 9 ψ, 9 χ1 and 4 χ2 angles for the Ref-1 peptide. The ^1H chemical shifts comprise 113 CαH protons, 67 methyl groups and 262 other non-exchangeable protons. [§]The improper torsion restraints serve to maintain planarity and chirality. All peptide bonds were constrained to be planar and *trans* with the exception of the peptide bond between Thr74 and Pro75 which is in the *cis* conformation. [#]E_{L-J} is the Lennard-Jones van der Waals energy calculated with the CHARMM [43] empirical energy function and is not included in the target function for simulated annealing or restrained minimization.

as the NFκB peptide binds in the opposite orientation to the Ref-1 peptide; see below. The disulfide-bonded cysteine [P$_0$] for NFκB is Cys62.) The structure of hTRX consists of a five-stranded β sheet (residues 1–5, 22–28, 53–59, 75–81 and 84–91) surrounded by four α helices (residues 7–17, 33–49, 62–70 and 94–105). The active site comprises a protrusion (residues 32–36) on the surface of the protein. The peptide binds in a crescent-shaped groove formed by residues in the active site, at the C terminus of strand β3, in helix 3, in the loop between helix 3 and strand β4, and in strand β5. The overall conformation

of the bound peptide is essentially extended and follows the shape of the cleft. At the N terminus of the peptide there is a helical turn from residues 61 to 64 with a hydrogen bond between thr61 O (the P$_{+4}$ position) and ile64 N (P$_{+1}$) as the peptide abuts the upper most point of the cleft. (Note that residues of hTRX and the peptide are distinguished by the first letter of the three-letter code, which is denoted by a capital and a small letter, respectively). In addition, there is another distorted helical turn from residues 66 to 69 with a hydrogen bond between ser66 O (P$_{-1}$) and val69 N (P$_{-4}$). This turn serves to orient val69 such that it can interact with the aromatic ring of Trp31.

The most remarkable feature of the complex is that the orientation of the Ref-1 peptide is opposite to that found in the complex with the target peptide from NFκB, although many of the interactions are preserved, as illustrated in Figures 4 and 5. Thus, the Ref-1 peptide is oriented antiparallel whereas the NFκB peptide is oriented parallel to residues 74–76 of hTRX. In both complexes, there are three intermolecular backbone–backbone hydrogen bonds involving Ala92 N, Thr74 O and Thr74 N of hTRX. Thus, the two intermolecular backbone–backbone hydrogen bonds involving Thr74 define the orientation of the peptide. In the case of Ref-1, these residues are hydrogen bonded to lys63 O (P$_{+2}$), cys65 N (P$_0$) and cys65 O (P$_0$), respectively; for NFκB they are hydrogen bonded to glu63 O (P$_{+1}$), glu63 N (P$_{+1}$) and val61 O (P$_{-1}$). It should be noted that the positions and orientations of cys65 NH (P$_0$) and cys65 O (P$_0$) in the Ref-1 peptide are essentially superimposable on those of glu63 N (P$_{+1}$) and val61 O (P$_{-1}$), respectively, in the NFκB peptide. In both cases, there is also an intermolecular hydrogen bond between the hydroxyl group of Thr74 of hTRX and the sulfur atom of the P$_0$ cysteine residue of the peptide. The majority of hydrophobic interactions are also preserved. Thus, the P$_{+3}$ residue interacts with Pro34; the P$_{+2}$ residue with Pro34 and Ala92; the P$_{+1}$ residue with Ser90 and Gly91; the P$_0$ residue with Trp31, Pro34 and Ala35; the P$_{-1}$ residue with Ala73; the P$_{-2}$ residue with Val59, Val71, Lys72, Ala73 and Lys74; and the P$_{-4}$ residue with Trp31. There are no cavities or unsatisfied hydrogen-bonding groups at the hTRX–peptide interface in either complex.

It is worth noting that the variant of hTRX employed in this study has a threonine at position 74 [20], whereas another variant has a methionine at this position [21]. This difference should have little effect on the hydrophobic interaction between the residue at position 74 and the aromatic ring at the P$_{-2}$ position (tryptophan in the case of Ref-1 and tyrosine for NFκB) [12].

The importance of hydrophobic interactions in stabilizing the formation of these complexes can be ascertained by calculating the solvation free energy (SFE) of folding [22]. Formation of the hTRX–Ref-1 complex is associated with

Figure 2
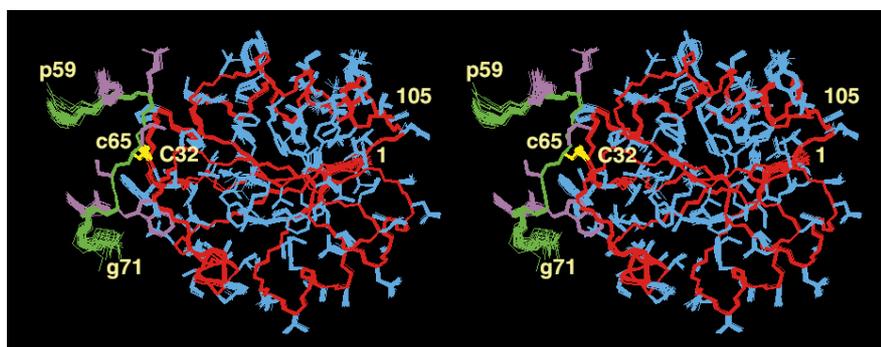
Stereoview showing a best fit superposition of the backbone (N, Cα, C) atoms and ordered side chains of the 35 simulated annealing structures of the hTRX–Ref-1 complex. The backbone and side chains of hTRX are shown in red and blue, respectively; the backbone and side chains of the Ref-1 peptide are shown in green and magenta, respectively; and the disulfide bond between Cys32 of hTRX and cys65 of the Ref-1 peptide is shown in yellow. Residues of hTRX and Ref-1 are distinguished by upper- and lower-case letters, respectively.

Table 2

Atomic rms differences (Å).*

	Backbone atoms	All atoms	All ordered atoms[†]
<SA> versus $\overline{SA}$	0.24±0.02	0.50±0.03	0.29±0.03
<SA> versus (SA)r	0.25±0.06	0.56±0.04	0.33±0.04
(SA)r versus $\overline{SA}$	0.067	0.27	0.15

*The notation of the structures is given in Table 1 footnote. [†]The coordinate precision is defined as the average atomic rms difference between the individual simulated annealing structures and the mean coordinates $\overline{SA}$. The values reported relate to residues 1–105 of hTRX and residues 61–69 of the Ref-1 peptide. The atoms that do not exhibit conformational disorder comprise all N, Cα, C, O and Cβ atoms of residues 1–105 of hTRX and 61–69 of the Ref-1 peptide; the complete hTRX side chains of residues 2, 5, 7–9, 10, 11, 14, 15, 17 to 19, 22–25, 27, 29–35, 38, 40–43, 45, 46, 49–55, 57, 59, 60, 62, 65–67, 69, 71, 73–80, 83, 86–92, 97 and 99–105; the complete side chains of the Ref-1 peptide excluding those of residues 59–60 and 70–71; and the hTRX side chains of Met1, Gln12, Ser28, Met37, Ser44 and Glu88 up to Cβ, Lys3, Glu6, Glu13, Asp16, Asp20, Asp26, Glu47, Asp58, Asp61, Asp64, Lys72, Gln84, Asn93, Lys94, Glu95 and Glu98 up to Cγ, and Gln4, Lys8, Lys21, Lys36, Lys39, Lys48, Glu56, Glu68, Glu70, Lys81, Lys85 and Lys96 up to Cδ.

a decrease of 624 Å^2 and 324 Å^2 in the solvent accessible surface area of the Ref-1 peptide and hTRX, respectively. This corresponds to an overall decrease in the calculated SFE of ~13 kcal mol^{-1}. Somewhat more accessible surface area is buried in the case of the hTRX–NFκB complex (768 Å^2 and 535 Å^2 for the peptide and protein, respectively), but the overall decrease (~12.5 kcal mol^{-1}) in the calculated SFE is essentially unchanged. Thus, both complexes should be very stable even in the absence of the formation of an intermolecular disulfide bridge.

Determinants of substrate orientation
How does hTRX recognize substrates in opposing orientations? We suggest that there are three discriminating interactions (all shown in Fig. 5). The first, and possibly the most important, discriminant is the presence of an aromatic residue at the P$_{-2}$ position (trp in the case of Ref-1 and tyr for NFkB). Upon complex formation, this residue becomes buried in a deep hydrophobic pocket. It is also possible for a long-chain hydrophobic such as ile or leu to occupy this position. The second is the presence of a hydrophobic residue at the P$_{-4}$ position, which interacts with the aromatic ring of Trp31. Finally, the third is the nature of the P$_{-5}$ residue. In the case of the NFκB the residue at P$_{-5}$ is a positively charged arginine permitting additional electrostatic interactions, in the form of two salt bridges with the side-chain carboxylates of Asp58 and Asp61. For the Ref-1 peptide, on the other hand, the P$_{-5}$ residue is negatively charged and precludes electrostatic interactions with hTRX beyond the P$_{-4}$ position. Thus, substrate side-chain interactions with hTRX determine the orientation of the peptide. The few main-chain interactions between hTRX and the two peptide substrates are centered around the intermolecular disulfide bond and do not have long-range asymmetry to discriminate between peptide orientations.

In considering the interaction of hTRX with target proteins, it is natural to ask oneself whether it is reasonable to expect the major determinants of binding to be located along a single peptide chain. Although it is clearly possible that contacts with other portions of the target proteins may occur, the results presented in this paper, as well as in the previous paper on the complex of hTRX with the NFκB peptide [12], strongly suggest that the major determinants are indeed located along a single peptide chain centered around the reactive cysteine of the target. Specifically, the similarities in the sequence dependence of certain key binding residues in the hTRX–Ref-1 and hTRX–NFκB peptide complexes support the assumption that these peptide model systems are actually representative of the real situation in the entire complex. This is further substantiated by the observation that in the X-ray structure of Anabena thioredoxin-2 binding occurs in the same orientation and location as for the NFκB peptide: the N-terminal residues of one molecule bind in the active-site region, parallel to residues 74–76 of another molecule [23]. Despite these structural arguments, it should be noted that no competition binding data are available which directly demonstrate that the Ref-1 peptide competes with full-length Ref-1.

Figure 3

Stereoview showing the interactions between the Ref-1 peptide and hTRX. The backbones (N, Cα, C) of hTRX and the Ref-1 peptide are shown in blue and red, respectively; the side chains of hTRX and the Ref-1 peptide at the interface of the complex are shown in magenta and green, respectively; and the disulfide bond between Cys32 of hTRX and cys62 of the Ref-1 peptide is shown in yellow. (The figure was generated with the program VISP [44].)
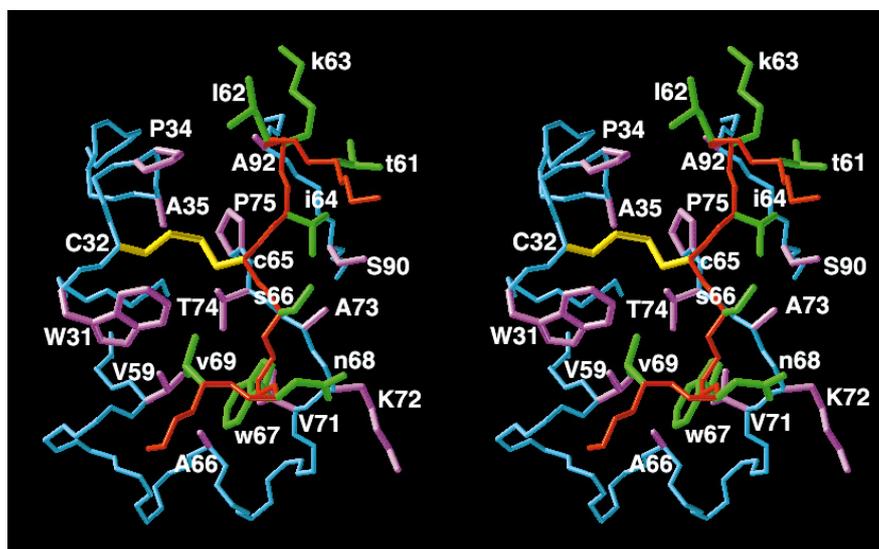
Antiparallel binding (i.e. in the same orientation as the Ref-1 peptide in the hTRX–Ref-1 complex) has been observed for the glutathione peptide in glutathione-binding proteins [24,25], and it has been proposed that a *cis*-proline (corresponding to residue 75 in hTRX) plays a major role in positioning the substrate for the thiol exchange reaction [26]. Indeed, examination of the position of the *cis* Pro75 ring in the structures of both the Ref-1 and NFκB peptide complexes reveals a strikingly similar arrangement for this side chain relative to the disulfide bond. The ring of Pro75 abuts, from one side, the sulfur of the P_0 cysteine in the bridge, presumably assuring the correct positioning of the sulfur of Cys32 for nucleophilic

attack by the resolving sulfhydryl anion, Cys35 (which is replaced by alanine in the complex described here).

The complexes of hTRX with target peptides from Ref-1 and NFκB represent only the second example of a protein recognizing peptides in distinct orientations. The other example is that of the recognition of polyproline-containing peptides by SH3 domains, in which the orientation is determined by the nature of the residues at the P_0 and P_{-3} positions [27–29]. However, in contrast to the SH3 domain, hTRX does not simply bind the target peptides but also carries out a chemical reaction. This involves nucleophilic attack by the highly reactive Cys32 thiolate

Figure 4

Comparison of **(a)** the hTRX–Ref-1 and **(b)** hTRX–NFκB peptide complexes. hTRX is represented as a molecular surface illustrating the cleft in which the two peptides, in their opposing orientations, are located. The degree of curvature of the molecular surface is color coded from white (convex) to dark grey (concave), and the N- and C-terminal ends of the two peptides are indicated in red lettering. The backbone of the peptides is shown in green, and side chains are colored as follows: cysteine, isoleucine, leucine, phenylalanine, proline, tyrosine and valine, yellow; arginine, blue; aspartate and glutamate, red; and asparagine, serine and threonine, magenta. (The figure was generated with the program GRASP [45].)
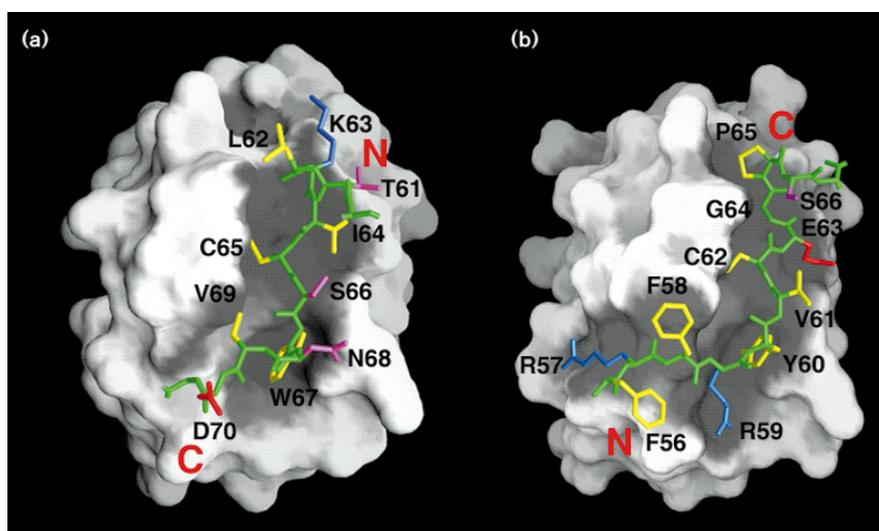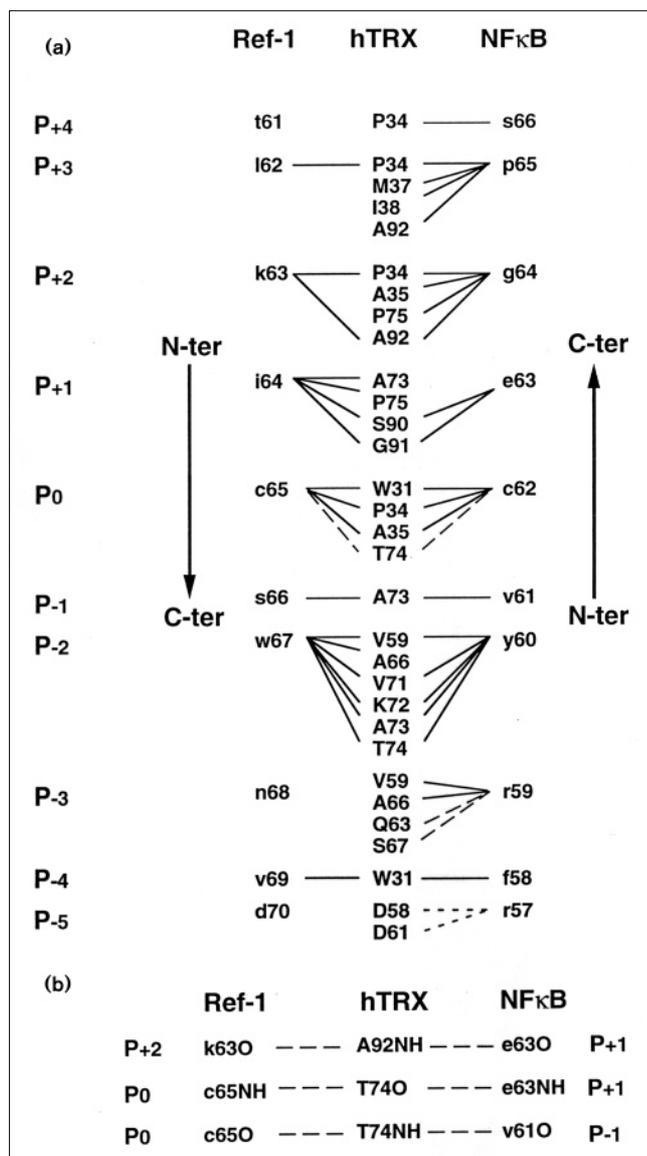
Figure 5

Schematic summary of the interactions observed in the hTRX–Ref-1 and hTRX–NFκB complexes. **(a)** All interactions with the exception of those involving backbone–backbone hydrogen bonds: hydrophobic, hydrogen-bonding and salt bridge interactions are represented by continuous (——), long dashed (– – –) and short dashed (---) lines, respectively. **(b)** Backbone–backbone hydrogen bonds.

at the P_{-1}, P_0, P_2 and P_3 sites pack in different ways depending upon the orientation of the peptide (internal, external, internal, external, respectively for one orientation; external, internal, external, internal, respectively, for the other orientation [27]).

To summarize, hTRX (as well as thioredoxins from other species) is distinct from most enzymes whose active site is located in a deep cleft. In hTRX, the active site is located on a protrusion of the molecular surface. The peptide substrates in the hTRX–Ref-1 and hTRX–NFκB complexes are wrapped around the protrusion of the reactive Cys32 in a crescent-shaped groove created by the backbone fold and side chains of hTRX. As a redox regulator for the cell, hTRX appears to have balanced versatility in substrate specificity with the requirements for access to substrates (some of which are known to be partially buried, such as the intersubunit disulfide of the NFκB p50 homodimer [30,31]).

Biological implications

The activation of a growing number of transcriptional and translational regulators has been shown to involve a thiol-redox control mechanism whereby specific cysteine residues are reduced by a cellular redox protein [3–11]. Human thioredoxin (hTRX) has been shown to play a key role in this process; it either interacts directly with these regulators, as in the case of the transcriptional factor NFκB and the translational regulator psbA mRNA protein complex, or via an indirect mechanism involving the intermediate redox protein Ref-1, as in the case of the transcriptional factor AP-1. An understanding of the molecular basis of this phenomenon requires the structure determination of cellular redox proteins in complexes with their targets [12].

We have previously solved the structure of a mixed (intermolecular) disulfide intermediate complex of hTRX and a 13-residue peptide comprising the target site of the p50 subunit of NFκB (residues 56–68). The complex is stabilized by numerous hydrogen-bonding, electrostatic and hydrophobic interactions, similar to those found in other high affinity protein–peptide complexes [12]. We have now determined the structure of a mixed disulfide intermediate complex of hTRX and a 13-residue peptide comprising the target site of Ref-1 (residues 59–71). Although the Ref-1 peptide is found in the same location as the NFκB peptide, that is, a crescent-shaped groove on the surface of hTRX, the surprising finding is that the orientation of the Ref-1 peptide is opposite to that of the NFκB peptide. (To facilitate discussion the residue numbering of the two peptides is denoted as follows: P_0 represents the disulfide-bonded cysteine; positive and negative numbers indicate residues N- and C-terminal to this cysteine, respectively, in the case of Ref-1, and C- and N-terminal to this cysteine,

anion of the reduced species of hTRX on a disulfide-containing substrate, producing a mixed disulfide intermediate. Attack by the thiolate of Cys35 then follows, yielding a reduced substrate and oxidized hTRX. Consequently, the environment surrounding the reactive Cys32 has to be nearly identical in the two complexes; the packing of the P_{+3} to P_{-4} residues are essentially the same in the hTRX–Ref-1 and hTRX–NFκB complexes, despite the opposing orientations of the peptide chain. Such stringency is not necessary in the SH3 case where the residues

respectively, in the case of NFκB as it binds in the opposite orientation to the Ref-1 peptide). Despite the differences in orientation, the environment surrounding the reactive Cys32 (which is responsible in the reduced species for nucleophilic attack on a disulfide-containing substrate, yielding a mixed disulfide intermediate) of hTRX, as well as the packing of the residues in the P_{-4} to P_{+3} positions, is very similar in the two complexes. Three discriminating interactions determine the orientation of the bound peptides: the presence of an aromatic (or possible long chain hydrophobic) residue at the P_{-2} position which is buried in a deep hydrophobic pocket; the presence of an aliphatic residue at the P_{-4} position to interact with the aromatic ring of Trp31 of hTRX; and the presence or absence of a positively charged residue at the P_{-5} position, to interact with the side-chain carboxylates of Asp58 and Asp61 of hTRX. The ability of hTRX to recognize peptides in opposing orientations indicates that this redox protein has succeeded in balancing versatility in substrate recognition with the requirements for access to substrates. Thereby, hTRX has the potential to target a wide range of proteins within the cell.

Materials and methods
Sample preparation
Uniformly labeled (>95%) ^{15}N and $^{15}N/^{13}C$ (Cys35→Ala, Cys62→Ala, Cys69→Ala and Cys73→Ala) quadruple mutant of hTRX was expressed and purified as described previously, using $^{15}NH_4Cl$ and $^{13}C_6$-glucose as the sole nitrogen and carbon sources, respectively [12,15]. The Ref-1 peptide $P_{59}ATLKICSWNVDG_{71}$ was synthesized using solid-phase methods and purified by HPLC using a C4-reversed phase column. Purity of the peptide was checked by mass spectrometry and NMR spectroscopy. The mixed disulfide intermediate complex between hTRX and the Ref-1 peptide was formed and purified exactly as described previously for the complex between hTRX and the NFκB peptide [12]. The purified complex was taken up in either 99.996% D_2O or 90% $H_2O/10\%$ D_2O.

NMR spectroscopy
All NMR experiments were carried out at 25°C on either a Bruker AMX600 or AMX500 spectrometer equipped with a z-shielded gradient triple resonance probe. The NMR spectra were processed with the NmrPipe package [32] and analysed using the programs PIPP, CAPP and STAPP [33]. Sequential assignment of the ^1H, ^{13}C and ^{15}N resonances, stereospecific assignments of β-methylene protons and methyls of leucine and valine, and the measurement of three-bond homonuclear and heteronuclear J couplings ($^3J_{HN\alpha}$, $^3J_{\alpha\beta}$, $^3J_{NH\beta}$, $^3J_{COH\beta}$, $^3J_{C\gamma N}$, $^3J_{C\gamma CO}$, $^3J_{CC}$) were achieved using the same set of 2D and 3D heteronuclear experiments described previously [12]. The ^1H resonances of the Ref-1 peptide were assigned using the conventional sequential assignment procedure using 2D $^{12}C(F_1,F_2)$-filtered HOHAHA and $^{12}C(F_1,F_2)$-filtered NOE spectra in D_2O, and $^{14}N/^{12}C(F_1,F_2)$-filtered NOE and $^{14}N(F_2)$-filtered COSY spectra in H_2O. Approximate interproton distance restraints were derived from the following NOE spectra recorded with a mixing time of 120 ms: 2D $^{12}C(F_1,F_2)$-filtered, $^{12}C/^{14}N(F_1,F_2)$-filtered and $^{14}N(F_2)$-filtered NOE spectra; 3D ^{15}N-edited, ^{13}C-edited and ^{13}C-edited$(F_2)/^{12}C$-filtered(F_3) NOE spectra; and 4D $^{15}N/^{13}C$-edited, $^{13}C/^{13}C$-edited NOE spectra. Details of all the NMR experiments employed, together with original references, are provided in [16–18,34]. The interproton distance restraints were grouped into four ranges: 1.8–2.7 Å (1.8–2.9 Å for NOEs involving NH protons), 1.8–3.3 Å (1.8–3.5 Å for NOEs involving NH protons), 1.8–5.0 Å, and 1.8–6.0 Å, corresponding to strong, medium, weak and very weak NOEs,

respectively. In addition, 0.5 Å was added to the upper limit of distances involving methyl protons to account for the higher apparent intensity of methyl resonances. Non-stereospecifically assigned methylene protons and methyl groups were treated as a $(\Sigma r^{-6})^{-1/6}$ sum [35]. Stereospecific assignments and ϕ, ψ and χ_1 torsion angle restraints were obtained using the conformational grid search program STEREOSEARCH on the basis of the $^3J_{HN\alpha}$ and $^3J_{\alpha\beta}$ coupling constants and intraresidue and sequential interresidue interproton distance restraints involving the NH, CαH and CβH protons [36]. Information from $^3J_{NH\beta}$ and $^3J_{COH\beta}$ coupling constants was also employed for identifying the appropriate χ_1 rotamer and for detecting rotamer averaging. χ_1 torsion angles for valine and threonine residues and stereospecific assignments for the methyl groups of valine residues were obtained from $^3J_{C\gamma N}$ and $^3J_{C\gamma CO}$ coupling constants, in conjunction with the pattern of intraresidue NOEs. χ_2 torsion angle restraints for isoleucine and leucine residues and stereospecific assignments for the methyl groups of leucine were obtained from $^3J_{CC}$ coupling constants and the pattern of intraresidue NOEs. Stereospecific assignments were obtained for 52 out of the 69 β-methylene groups, all methyl groups of the 6 leucine and 10 out of 11 valine residues of hTRX, 7 out of 8 β-methylene groups and the methyl groups of the single leucine residue of the Ref-1 peptide.

Structure calculations
The structures were calculated using the hybrid distance geometry-simulated annealing protocol [37] which makes use of the program XPLOR-31 [38]. The target function that is minimized during simulated annealing (SA) comprises quadratic harmonic potential terms for covalent geometry (that is bonds, angles, planes and chirality), square-well quadratic potentials for the experimental distance and torsion angle restraints, harmonic potentials for the $^3J_{HN\alpha}$ coupling constant [39], $^{13}C\alpha$ and $^{13}C\beta$ secondary chemical shift [40] and ^1H chemical shift [41] restraints, and a quartic van der Waals repulsion term for the non-bonded contacts. In addition, a conformational database potential term [42] was included to restrict sampling during simulated annealing refinement to conformations that are likely to be energetically possible, thereby limiting the choices of dihedral angles to those that are known to be physically realizable; in this manner the variability in the structures is primarily the result of the experimental restraints, rather than an artifact of a poor non-bonded interaction model [42]. No hydrogen-bonding, electrostatic or 6–12 Lennard-Jones empirical potential energy terms are present in the target function. The $^3J_{HN\alpha}$ coupling constants included directly in the refinement comprised only those that could be measured from the 3D HNHA experiment to an accuracy of 0.5 Hz or better. The minimum ranges employed for the ϕ, ψ, χ_1 and χ_2 torsion angle restraints were ±10°, ±50°, ±20° and ±20°, respectively. The narrow range for some of the ϕ restraints was made possible by the availability of highly accurate $^3J_{HN\alpha}$ coupling constant data. The χ_2 angles of all tyrosine and phenylalanine aromatic rings were restrained to 90±30°. In all cases the angular standard deviations of the torsion angles for the ensemble of 35 final SA structures were much smaller than the ranges employed for the corresponding torsion angle restraints. Only structurally useful intraresidue NOEs were included in the intraresidue interproton distance restraints. Thus, NOEs between protons separated by two bonds or between non-stereospecifically assigned protons separated by three bonds were not incorporated in the restraints. Hydrogen bonding restraints, which account for all the slowly exchanging backbone amide protons, were only included in the final stages of refinement. For each backbone hydrogen bond there are two distance restraints: r_{NH-O}, 1.7–2.5 Å; r_{N-O}, 2.3–3.5 Å. (Note that these distance criteria were also used to assess the presence of intermolecular hydrogen bonds between hTRX and the Ref-1 peptide).

Accession numbers
The coordinates of the 35 final simulated annealing (SA) structures of the hTRX–Ref-1 complex, together with the coordinates of the restrained regularized mean structure, $\overline{(SA)}r$, and the experimental restraints have been deposited in the Brookhaven Protein Databank (accession number 1CQG). The coordinates can also be obtained by e-mail from GMC at clore@vger.niddk.nih.gov.

References

1. Holmgren, A. (1995). Thioredoxin structure and mechanism: conformational changes on oxidation of the active-site sulfhydryls to a disulfide. *Structure* **3**, 239–243.

2. Martin, J.L. (1995). Thioredoxin: a fold for all reasons. *Structure* **3**, 245–250.

3. Matthews, J.R., Wakasugi, N., Virelizier, J.L., Yodoi, J. & Hay, R.T. (1992). Thioredoxin regulates the DNA binding activity of NFκB by reduction of a disulfide bond involving cysteine 62. *Nucleic Acids Res.* **20**, 3821–3830.

4. Hayashi, T., Ueno, Y. & Okamoto, T. (1993). Oxidoreductive reductive regulation of nuclear factor κB. *J. Biol. Chem.* **268**, 11380–11388.

5. Mitomo, K., Nakayama, K., Fujimoto, K., Sun, X., Seki, S. & Yamamoto, K. (1994). Two different cellular redox systems regulate the DNA-binding activity of the p50 subunit of NF-κB *in vitro*. *Gene* **145**, 197–203.

6. Deiss, L.P. & Kimchi, A. (1991). A genetic tool used to identify thioredoxin as a mediator of a growth inhibitor signal. *Science* **252**, 117–120.

7. Meyer, M., Schreck, R. & Baeuerle, P.A. (1992). H_2O_2 and antioxidants have opposite effects on the activation of NF-κB and AP-1 in intact cells: AP-1 as secondary antioxidant-responsive factor. *EMBO J.* **12**, 2005–2015.

8. Abate, C., Patel, L., Rauscher, F.J. & Curran, T. (1990). Redox regulation of Fos and Jun DNA-binding activity *in vitro*. *Science* **249**, 1157–1161.

9. Xanthoudakis, S., Miao, G., Wang, F., Pan, Y.-C.E. & Curran, T. (1992). Redox activation of Fos-Jun DNA binding activity is mediated by a DNA repair enzyme. *EMBO J.* **11**, 3323–3335.

10. Danon, A. & Mayfield, S.P. (1994). Light-regulated translation of chloroplast messenger RNAs through redox potential. *Science* **266**, 1717–1719.

11. Levings, C.S. & Siedow, J.N. (1995). Regulation by redox poise in chloroplasts. *Science* **268**, 695–696.

12. Qin, J., Clore, G.M., Kennedy, W.M.P, Huth, J.R. & Gronenborn, A.M. (1995). Solution structure of human thioredoxin in a mixed disulfide intermediate complex with its target peptide from the transcription factor NFκB. *Structure* **3**, 289–297.

13. Walker, L.J., Robson, C.N., Black, E., Gillespie, D. & Hickson, I.D. (1993). Identification of residues in the human DNA repair enzyme HAP1 (Ref-1) that are essential for redox regulation of Jun DNA binding. *Mol. Cell. Biol.* **13**, 5370–5376.

14. Xanthoudakis, S., Miao, G.G. & Curran, T. (1994). The redox and DNA-repair activities of Ref-1 are encoded by nonoverlapping domains. *Proc. Natl. Acad. Sci. USA* **91**, 23–27.

15. Qin, J., Clore, G.M. & Gronenborn, A.M. (1994). The high-resolution three-dimensional solution structures of the oxidized and reduced states of human thioredoxin. *Structure* **2**, 503–521.

16. Clore, G.M. & Gronenborn, A.M. (1991). Structures of larger proteins in solution: three- and four-dimensional heteronuclear NMR spectroscopy. *Science* **252**, 1390–1399.

17. Bax, A. & Grzesiek, S. (1993). Methodological advances in protein NMR. *Accounts Chem. Res.* **26**, 131–138.

18. Gronenborn, A.M. & Clore, G.M. (1995). Structures of protein complexes by multidimensional heteronuclear magnetic resonance spectroscopy. *CRC Crit. Rev. Biochem. Mol. Biol.* **30**, 351–385.

19. Laskowski, R.A., MacArthur, M.W., Moss, D.S. & Thornton, J.M. (1993). PROCHECK: a program to check the stereochemical quality of protein structures. *J. Appl. Cryst.* **26**, 283–291.

20. Wollman, E.E., *et al.*, & Fradelizi, D. (1988). Cloning and expression of a cDNA for human thioredoxin. *J. Biol. Chem.* **263**, 15506–15512.

21. Tagaya, Y., *et al.*, & Yodoi, J. (1989). ATL-derived factor (ADF), an IL-2 receptor/Tac inducer homologous to thioredoxin; possible involvement of dithio-reduction in the IL-2 receptor induction. *EMBO J.* **8**, 7357–7364.

22. Eisenberg, D. & McLaghlan, A.D. (1986). Solvation energy in protein folding and binding. *Nature* **319**, 199–203.

23. Saarinen, M., Gleason, F.K. & Eklund, H. (1995). Crystal structure of thioredoxin-2 from *Anabaena. Structure* **3**, 1097–1108.

24. Sinning, I., *et al.*, & Jones, T.A. (1993). Structure determination and refinement of human alpha class glutathione transferase A1-1, and a comparison with the Mu and Pi class enzymes. *J. Mol. Biol.* **232**, 192–212.

25. Bushweller, J.H., Billeter, M., Holmgren, A. & Wüthrich, K. (1994). The nuclear magnetic resonance solution structure of the mixed disulfide between *Escherichia coli* glutaredoxin (C14S) and glutathione. *J. Mol. Biol.* **235**, 1585–1597.

26. Nikkola, M., Gleason, F., Saarinen, M., Joelson, T., Björnberg, O. & Eklund, H. (1991). A putative glutathione binding site in T4 glutaredoxin investigated by site-directed mutagenesis. *J. Biol. Chem.* **266**, 16105–16112.

27. Lim, W.A., Richards, F.M. & Fox, R.O. (1994). Structural determinants of peptide-binding orientation and of sequence specificity in SH3 domains. *Nature* **372**, 375–379.

28. Feng, S., Chen, J.K., Yu, H., Simon, J.A. & Schreiber, S.L. (1994). Two binding orientations for peptides to the Src SH3 domain: development of a general model for SH3–ligand interactions. *Science* **266**, 1241–1247.

29. Wu, X., *et al.*, & Kuriyan, J. (1995). Structural basis for specific interaction of lysine-containing proline-rich peptides with the N-terminal SH3 domain of c-Crk. *Structure* **3**, 215–226.

30. Ghosh, G., Duyne, G.V., Ghosh, S. & Sigler, P.B. (1995). The structure of NFκB.p50 homodimer bound to a κB site. *Nature* **373**, 303–310.

31. Müller, G.W., Rey, F.A., Sodeoka, M., Verdine, G.L. & Harrison, S.C. (1995). Structure of the NF-κB homodimer bound to DNA. *Nature* **373**, 311–317.

32. Delaglio, F., Grzesiek, S., Vuister, G.W., Zhu, G., Pfeifer, J. & Bax, A. (1995). NMRPipe: a multidimensional spectral processing system based on UNIX pipes. *J. Biomol. NMR* **6**, 277–293.

33. Garrett, D.S., Powers, R., Gronenborn, A.M. & Clore, G.M. (1991). A common sense approach to peak picking in two-, three-, and four-dimensions using automatic computer analysis of contour diagrams. *J. Magn. Reson.* **95**, 214–220.

34. Bax, A., *et al.*, & Zhu, G. (1994). Measurement of homo- and heteronuclear *J* couplings from quantitative *J* correlation spectroscopy. *Methods Enzymol.* **239**, 79–106.

35. Nilges, M. (1993). A calculational strategy for the structure determination of symmetric dimers by ^{1}H NMR. *Proteins* **17**, 297–309.

36. Nilges, M., Clore, G.M. & Gronenborn, A.M. (1990). ^{1}H-NMR stereospecific assignments by conformational database searches. *Biopolymers* **29**, 813–822.

37. Nilges, M., Clore, G.M. & Gronenborn, A.M. (1988). Determination of three dimensional structures of proteins from interproton distance data by hybrid distance geometry-dynamical simulated annealing calculations. *FEBS Lett.* **229**, 317–324.

38. Brünger, A.T. (1992). *X-PLOR Version 3.1: A System for X-ray Crystallography and NMR*. Yale University Press, New Haven, CT.

39. Garrett, D.S., *et al.*, & Clore, G.M. (1994). The impact of direct refinement against three bond HN-CαH coupling constants on protein structure determination by NMR. *J. Magn. Reson. B* **104**, 99–103.

40. Kuszewski, J., Qin, J., Gronenborn, A.M. & Clore, G.M. (1995). The impact of direct refinement against [13]Cα and [13]Cβ chemical shifts on protein structure determination by NMR. *J. Magn. Reson. B* **106**, 92–96.

41. Kuszewski, J., Gronenborn, A.M. & Clore, G.M. (1995). The impact of direct refinement against proton chemical shifts on protein structure determination by NMR. *J. Magn. Reson. B* **107**, 293–297.

42. Kuszewski, J., Gronenborn, A.M. & Clore, G.M. (1996). Improving the quality of NMR and crystallographic protein structures by means of a conformational database potential derived from structure databases. *Protein Sci.*, in press.

43. Brooks, B.R., *et al.*, & Karplus, M. (1983). CHARMM: a program for macromolecular energy minimization and dynamics calculations. *J. Comput. Chem.* **4**, 187–217.

44. De Castro, E. & Edelstein, S. (1992). *VISP 1.0 User's Guide*. University of Geneva, Switzerland.

45. Nicholls, A.J., Sharp, K. & Honig, B. (1991). Protein folding and association: insights from interfacial and thermodynamic properties of hydrocarbons. *Proteins* **11**, 281–296.